Long-range Brillouin optical time-domain analysis sensor employing pulse coding techniques

2010 Meas. Sci. Technol. 21 094024

(http://iopscience.iop.org/0957-0233/21/9/094024)

Meas. Sci. Technol. **21** (2010) 094024 (7pp) doi:10.1088/0957-0233/21/9/094024

Long-range Brillouin optical time-domain analysis sensor employing pulse coding techniques

Marcelo A Soto[1,2], Gabriele Bolognini[2], Fabrizio Di Pasquale[2] and Luc Thévenaz[1]

[1] EPFL Swiss Federal Institute of Technology, Institute of Electrical Engineering, Group for Fibre Optics, STI IEL GR-SCI Station 11, CH-1015 Lausanne, Switzerland
[2] Scuola Superiore Sant'Anna, via G Moruzzi 1, 56124 Pisa, Italy

E-mail: m.soto@sssup.it

Received 14 January 2010, in final form 14 April 2010
Published 28 July 2010
Online at stacks.iop.org/MST/21/094024

Abstract
In this paper we describe and implement a long-range Brillouin optical time-domain analysis (BOTDA) sensor, for both temperature and strain measurements, using optical pulse coding techniques. A theoretical analysis of Simplex coding applied to BOTDA systems is presented and experimentally demonstrated for both Brillouin loss and Brillouin gain configurations. With the proposed technique, ∼7.1 dB and ∼10.3 dB of signal-to-noise ratio improvements are demonstrated in BOTDA measurements using 127-bit and 511-bit Simplex codes, respectively. This feature allows us to extend the dynamic range of the measurements, overcoming the limitations to the maximum usable optical power imposed by pump depletion and modulation instability; thus, the sensing range can be extended by several tens of kilometers while keeping meter-scale spatial resolution. Experimental results show the capabilities of optical pulse coding techniques to achieve 1 m spatial resolution over 50 km of standard single-mode fiber enabling temperature and strain resolutions equal to 2.2 °C and 44 $\mu\varepsilon$, respectively.

Keywords: optical fiber sensors, stimulated Brillouin scattering, fiber testing, coding

1. Introduction

Fiber optic sensors based on stimulated Brillouin scattering (SBS) have attracted a great deal of attention in recent years, thanks to their unparalleled ability to continuously measure a physical variable of interest, such as strain or temperature, along an optical fiber [1, 2]. The typical detection technique used in SBS-based sensors refers to the so-called Brillouin optical time-domain analysis (BOTDA) technique [1, 3], which is based on the use of an optical pulse acting as a pump signal and a counter-propagating continuous-wave (CW) probe beam. Thus, by measuring variations of the Brillouin gain spectrum (BGS) [4] along an optical fiber, distributed strain and temperature measurements can be carried out. The spatial resolution is given by the pump pulse duration, and is ultimately limited to 1 m, corresponding to 10 ns pulse duration, when using standard BOTDA techniques. When aiming at long-range measurements with meter-scale spatial resolution [5, 6], the short SBS interaction results in a weak measured signal, offering poor accuracy when measuring the BGS. On the other hand, a strong probe signal can induce pump depletion [3] or modulation instability [7], reducing the interaction between the pump and probe signal due to gain saturation. In order to avoid such nonlinear effects, both the pump and probe powers must be kept below given thresholds; the maximum power constraint actually constitutes the main limiting factor to the sensing distance in long-range BOTDA-based sensors [5, 6]. The best performance experiments reported so far for long-range BOTDA-based sensors have resulted in 2 m/5 m spatial resolution over 40 km/51 km of standard single-mode fiber (SSMF) [5, 6].

In this paper we present a detailed analysis of the use of optical pulse coding techniques [8, 9] to extend the sensing range of BOTDA sensors while keeping meter-scale spatial resolution. This technique has been demonstrated to provide an enhanced signal-to-noise ratio (SNR), extending the sensing range of simultaneous strain and temperature measurements based on spontaneous Brillouin scattering [10]. In principle, then, by applying pulse coding, the interaction between pump and probe signals in BOTDA sensors can be effectively increased [11, 12], thus overcoming the typical trade-off between spatial resolution and sensing range. This possibility has been recently implemented and early results have been obtained in long-range as well as short-range sensors [11–13]. In this paper we present a detailed theoretical analysis of optical pulse coding techniques applied to BOTDA sensors, providing a thorough investigation of the underlying assumptions, followed by relevant experimental tests aimed at implementing and validating the proposed technique.

This paper is organized as follows: first, the theory of optical pulse coding techniques applied to BOTDA sensors is analyzed. Then, the experimental setup and results are presented, demonstrating the feasibility of using this technique to significantly extend the sensing range while keeping 1 m spatial resolution. The experimental demonstration of 1 m spatial resolution over 50 km sensing distance is then described in detail, representing the best performance reported so far, to our knowledge, in long-range BOTDA sensors. Finally the conclusions are presented.

2. Theory

In BOTDA sensors, a single-mode optical fiber is used as a distributed amplifier, where a pump wave transfers part of its energy to a counter-propagating probe signal through the interaction with acoustic phonons [1–3]. The probe–pump interaction actually creates a periodic perturbation of the refractive index of the fiber, thus reflecting part of the pump signal by Bragg diffraction and reinforcing the acoustic wave. This energy transfer takes place at any fiber position when the frequency difference between the optical waves is within the local BGS [4]. The maximum amplification occurs when the frequency offset between the two optical waves equals the peak acoustic-phonon frequency. This frequency is called the Brillouin frequency shift (BFS) and depends linearly on strain and temperature [1], providing an effective mechanism to perform the distributed sensing of these physical quantities along an optical fiber. Thus, the BFS change ($\Delta\nu_B$) along the fiber can be expressed as a linear combination of temperature variation (ΔT) and strain variation ($\Delta\varepsilon$), as follows:

$$\Delta\nu_{\mathrm{B}} = C_{\nu_{\mathrm{B}}\varepsilon} \cdot \Delta\varepsilon + C_{\nu_{\mathrm{B}}T} \cdot \Delta T, \qquad (1)$$

where $C_{\nu_{\mathrm{B}}\varepsilon} = 0.048$ MHz $\mu\varepsilon^{-1}$ and $C_{\nu_{\mathrm{B}}\mathrm{T}} = 1.07$ MHz $^{\circ}\mathrm{C}^{-1}$ are the strain and temperature coefficients for BFS in silica fibers [10]. Depending on the measurement configuration, a continuous-wave probe signal can be launched at the fiber end ($z = L$) with either a down-shifted frequency (in the so-called Brillouin gain configuration [3, 5]) or an up-shifted frequency (in the so-called Brillouin loss configuration [2]) with respect to the pump frequency. In order to measure the BGS along the fiber, the frequency difference between the pump and probe is swept around the BFS, i.e. around ∼10.9 GHz at 1550 nm in standard single-mode fibers at room temperature and zero-strain applied [5]. In BOTDA sensors, the spatial resolution is obtained by using a pulsed pump signal (launched at the fiber input, $z = 0$) and the local BFS is measured by sweeping the frequency offset within a range of some hundreds of MHz around the BFS. Thus, in order to reconstruct the Brillouin gain spectrum along the fiber, variations on the CW probe signal intensity (ΔI_{CW}) are measured at the fiber input ($z = 0$) as a function of time, t, and for different frequency offset, $\Delta\nu$ [3]:

$$\Delta I_{\mathrm{CW}}(t, \Delta\nu) = I_{\mathrm{CWL}} \exp(-\alpha L)\{G(t, \Delta\nu) - 1\}, \qquad (2)$$

where I_{CWL} is the input probe intensity at the far end of the fiber ($z = L$), α is the fiber loss, L is the fiber length and $G(t, \Delta\nu)$ is the Brillouin gain defined as

$$G(t, \Delta\nu) = \exp\left[\int_{v_g t/2}^{v_g t/2+\Delta z} g_B(\xi, \Delta\nu) I_P(\xi, \Delta\nu)\,\mathrm{d}\xi\right], \qquad (3)$$

where v_g is the group velocity, Δz is the spatial resolution given by the pump pulse duration, and $g_B(\xi, \Delta\nu)$ and $I_P(\xi, \Delta\nu)$ are the BGS and the pump intensity at position $z = \xi$. Neglecting pump depletion, the expression for the pump intensity simplifies to $I_{P0}\exp(-\alpha\xi)$, where I_{P0} is the input pump intensity [3]. From equations (2) and (3) we can note that when using short pulses, a short pump–probe interaction length takes place; as a consequence, the CW-intensity contrast decreases, reducing the SNR of the measurement [5, 6]. Although equation (3) points out that the pump power could be increased in order to extend the sensing range, the maximum pump and probe powers are however limited by pump depletion [3] and modulation instability [7], effects which induce distortion in the reconstructed BGS. In fact, when using high pump power, the local pump intensity along the fiber, $I_P(\xi, \Delta\nu)$, depends on the Brillouin interaction at every preceding position, inducing significant deviation of the measured BGS peak frequency with respect to the real local value [3]. This feature leads to systematic errors in the strain and temperature measurements, which increase with the distance and optical power. Taking into account this upper limitation on the maximum pump and probe powers, the SNR cannot be effectively enhanced when maintaining a given spatial resolution. The sensing range could be increased by using longer pump pulses, enhancing the SNR but negatively affecting the achievable spatial resolution [5, 6]. Thus, these non-local effects, as well as modulation instability, result in the main limitations on the maximum sensing distance in long-range BOTDA sensors [5, 6].

An alternative that we propose here to improve the SNR of the measured BOTDA traces is the use of optical pulse coding techniques, such as for instance Simplex coding [8–10]. It has been recently demonstrated that the use of pulse coding allows for an extended sensing range in simultaneous strain and temperature measurements based on spontaneous Brillouin scattering [10]. One of the limitations of Simplex coding is related to its linear properties, which in principle could make it inapplicable to nonlinear systems such as distributed Brillouin amplifiers, with a SBS gain represented by equation (3). However, considering that the interaction length in BOTDA sensors is very short, the Brillouin gain is

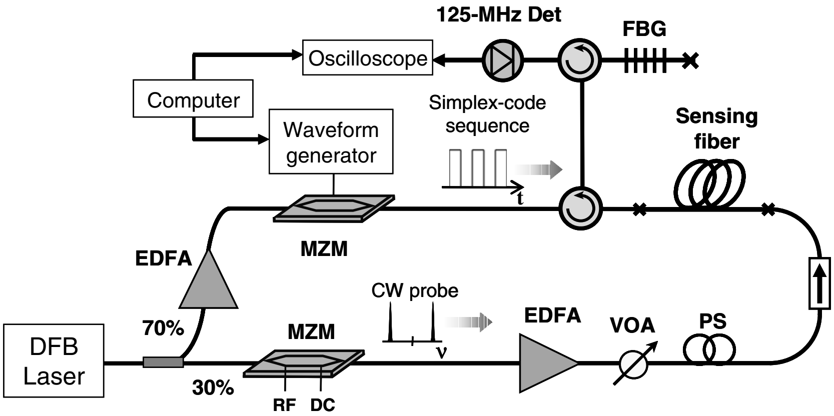

Figure 1. Simplex-coded BOTDA-based sensor.

actually very small, i.e.

$$\int_{v_g t/2}^{v_g t/2+\Delta z} g_B(\xi, \Delta\nu) I_P(\xi, \Delta\nu)\, \mathrm{d}\xi \ll 1, \quad (4)$$

so that the Brillouin gain can be approximately considered as a linear process, and the expression for ΔI_{CW} can be linearized as

$$\Delta I_{\mathrm{CW}}\,(t, \Delta\nu) \propto \int_{v_g t/2}^{v_g t/2+\Delta z} g_B(\xi, \Delta\nu) I_P(\xi, \Delta\nu)\, \mathrm{d}\xi. \quad (5)$$

Taking into account the linear dependence of ΔI_{CW} on the pump intensity $I_P(\xi, \Delta\nu)$, the SNR of the measurement can thus be effectively enhanced by using linear optical pulse coding [8–10], such as Simplex coding, without affecting the spatial resolution. Note that when using pulse coding, the interaction length actually depends on the code length (L_c), i.e. the number of bits used in Simplex coding, so that the CW-intensity contrast can be expressed as

$$\Delta I_{\mathrm{CW}}(t, \Delta\nu) \propto \sum_{i=1}^{Lc} \int_{v_g t/2+(i-1)\Delta z}^{v_g t/2+i\Delta z} g_B(\xi, \Delta\nu) I_{Pi}(\xi, \Delta\nu)\, \mathrm{d}\xi, \quad (6)$$

where $I_{Pi}(\xi, \Delta\nu)$ is the pump intensity of the ith bit at a distance $z = \xi$, and a frequency offset $\Delta\nu$. This equation clearly points out that the measured ΔI_{CW}, when using coding, corresponds to a linear combination of the several pulses composing the Simplex-coded pump signal. This feature allows us to use the conventional linear decoding process for Simplex codes without any modification [8]. Thus, the coded-BOTDA traces measured at the fiber input ($z = 0$) can be represented by the following expression:

$$\begin{pmatrix} \eta_1(t) \\ \vdots \\ \eta_i(t) \\ \vdots \\ \eta_{Lc}(t) \end{pmatrix} = S \begin{pmatrix} \psi_1(t) \\ \vdots \\ \psi_i(t) \\ \vdots \\ \psi_{Lc}(t) \end{pmatrix} + \begin{pmatrix} e_1(t) \\ \vdots \\ e_i(t) \\ \vdots \\ e_{Lc}(t) \end{pmatrix}, \quad (7)$$

where $\eta_i(t)$ is the ith coded-BOTDA trace (with $i \in [1, L_c]$), $\psi_i(t)$ is the single-pulse BOTDA trace delayed in an ith multiple of the bit duration with respect to $\psi_1(t)$, and $e_i(t)$ is the amplitude of the uncorrelated zero-mean noise added to the measurement of the ith coded-BOTDA trace [8, 9]. The decoding process can be carried out by linear processing of the traces as follows:

$$\begin{pmatrix} \widehat{\psi}_1(t) \\ \vdots \\ \widehat{\psi}_i(t) \\ \vdots \\ \widehat{\psi}_{Lc}(t) \end{pmatrix} = S^{-1} \begin{pmatrix} \eta_1(t) \\ \vdots \\ \eta_i(t) \\ \vdots \\ \eta_{Lc}(t) \end{pmatrix}, \quad (8)$$

where $\widehat{\psi}_i(t)$ is the estimated single-pulse BOTDA trace $\psi_i(t)$. After inversely time-shifting the estimated BOTDA traces and averaging them, the final decoded trace has an SNR better than the one obtained by a conventional single-pulse measurement, considering the same number of acquisitions, i.e. the same measurement time [8, 9]. The SNR enhancement in BOTDA traces is quantified by the coding gain defined as [9]

$$G_{\mathrm{cod}} = \frac{L_c + 1}{2\sqrt{L_c}}. \quad (9)$$

Thus, with such SNR enhancement, optical pulse coding allows us to notably increase the frequency accuracy ($\delta\nu_B$) when reconstructing the BFS. The BFS accuracy actually depends on the electrical SNR value according to the following expression:

$$\delta\nu_B = \frac{\Delta\nu_B}{\sqrt{2}(\mathrm{SNR})^{1/4}}, \quad (10)$$

where $\Delta\nu_B$ is the Brillouin light linewidth [1]. Hence, one major benefit of optical pulse coding in BOTDA sensors is that the SNR enhancement allows us to increase the dynamic range of the measured BOTDA traces, overcoming the trade-off between spatial resolution and sensing distance, and resulting then in an extended sensing range while ensuring high spatial resolution.

3. Experimental setup

The experimental setup used to evaluate the impact of pulse coding on a BOTDA sensor is similar to a conventional BOTDA scheme [5], and is shown in figure 1. The light

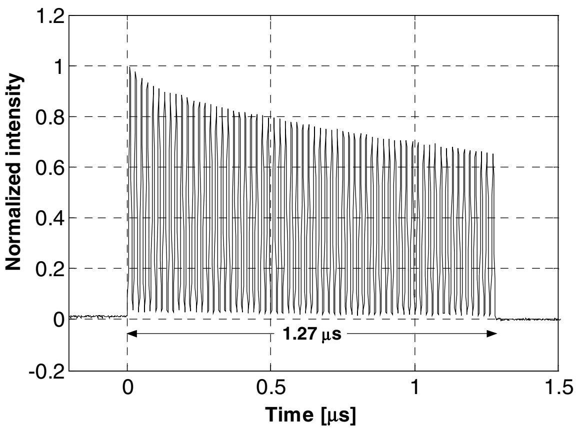

Figure 2. Measured single 127-bit Simplex codeword amplified by an EDFA.

source corresponds to a standard distributed-feedback (DFB) laser operating at 1535 nm and with ∼10 dBm output power. The CW-light is first divided into pump and probe branches using a 70/30 optical splitter. One of the outputs of the splitter (70% output) is used as a pump signal while the 30% output is used as a probe signal. The main modification of the setup, with respect to a conventional BOTDA sensor, concerns the generation of the pulsed pump, while in conventional BOTDA the Mach–Zehnder modulator (MZM) used for pulse shaping is generally placed before an erbium-doped optical amplifier (EDFA) in order to increase the peak pump power; in our implementation the MZM is instead situated after the EDFA avoiding distortion of the Simplex-coded pulses due to gain saturation of the EDFA. The MZM is controlled by an arbitrary waveform generator to produce either single pulses or Simplex-coded pulses, with a pulse duration of 10 ns, allowing for 1 m spatial resolution. The code length employed in our experiments was up to 511 bit, with codeword repetition rate slightly lower than 2 kHz; a spatial resolution of 1 m was achieved without penalties in the decoded trace. The limitations to the use of longer code sequences in our case are mainly given by possible saturation-induced issues at the receiver side.

Note that, if pulse coding is implemented in a conventional setup of a BOTDA-based sensor, with the EDFA placed after the MZM, the distortion produced by the gain saturation of the EDFA would significantly impact on the performance of the pulse coding technique. As an example, figure 2 shows a 127-bit Simplex-coded sequence affected by the transient of the EDFA. It is evident that the amplitudes of all bits within a single codeword, as well as in different codewords, are different. This feature does not satisfy the power uniformity requirement imposed on $\psi_i(t)$ in equation (7) in order to be able to perform linear decoding. If such distorted sequences of pulses are used in a coded-BOTDA sensor, the decoding process would need to take into account the individual codeword shapes, which depend on the actual saturation conditions of the used EDFA, resulting in an impractical solution for a real sensor. On the other hand, placing the EDFA before the MZM allows us to generate undistorted coded-pulse sequences with a uniform peak pulse power, but with a reduced power level

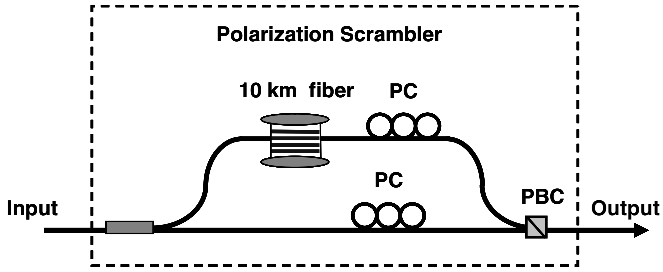

Figure 3. Passive polarization scrambler.

(∼15 dBm at the fiber input). However, taking into account that pump depletion and modulation instability limit the maximum pump peak power in long-range BOTDA sensors [3, 7], this modification actually does not represent a significant penalty for the system, while it is essential to keep the original properties of the code, allowing us to perform a linear decoding without any modification.

In the probe branch (30% output of the splitter), the CW-light at 1535 nm is intensity modulated using a MZM controlled by a microwave (RF) generator, producing two sidebands around the laser frequency with a highly suppressed carrier when the dc voltage is properly set [4, 5]. Thus, the BGS along the fiber is scanned sweeping the frequency of the microwave signal at around the BFS. These two modulation sidebands are first amplified by an EDFA, followed by a variable optical attenuator (VOA) to properly set the probe power level sent into the fiber to −13 dBm per sideband.

On the other hand, considering that the efficiency of SBS critically depends on the state of polarization of the probe and pump signals, a polarization scrambler (PS) has been used to depolarize the probe light. Figure 3 shows the implemented passive PS which is composed of a splitter, two polarization controllers, a few km of SSMF and a polarization beam combiner (PBC). Note that the length difference of the two arms is larger than the coherence length of the laser, so that both optical beams are combined incoherently at the output of the PBC. By adjusting both polarization controllers, the two orthogonal polarization components are combined with the same power level at the output of the PBC, ensuring uniform scrambling of the probe. Thus, fluctuations of the Brillouin gain due to polarization changes along the fiber are highly suppressed. Probe and pump signals are then launched in counter-propagating directions into a 50 km SSMF. Although both sidebands of the probe are launched into the fiber and extracted at one of the fiber ends using an optical circulator, only the Stokes component is selected by a narrowband fiber Bragg grating (FBG, <0.1 nm), and then detected by a 125 MHz photodiode, connected to an oscilloscope controlled by a computer. Note that the propagation of both sidebands along the fiber reduces pump depletion and non-local effects [14], alleviating the possible additional pump depletion introduced by Simplex coding in long-range BOTDA sensors.

4. Results

Considering that equations (2)–(6) describing the SBS process can be effectively used to model Brillouin gain as well

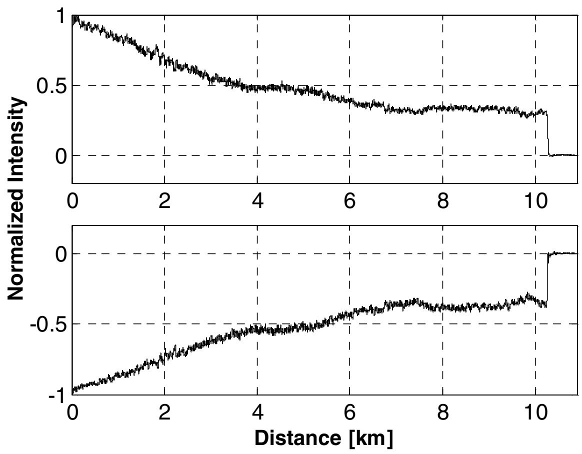

Figure 4. Decoded BOTDA traces (*a*) using Brillouin gain configuration and (*b*) using Brillouin loss configuration.

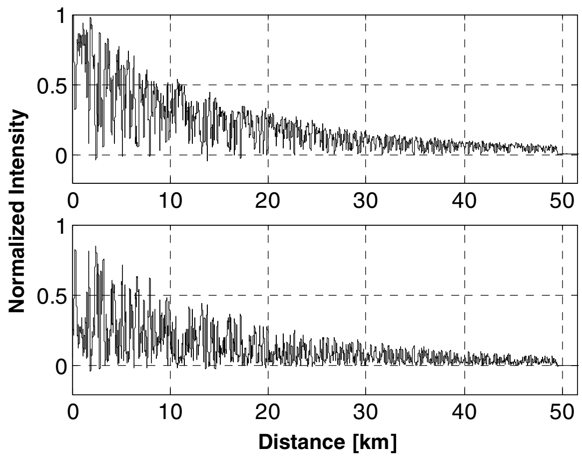

Figure 5. Decoded BOTDA traces for 50 km of fiber, with orthogonally polarized probe signals.

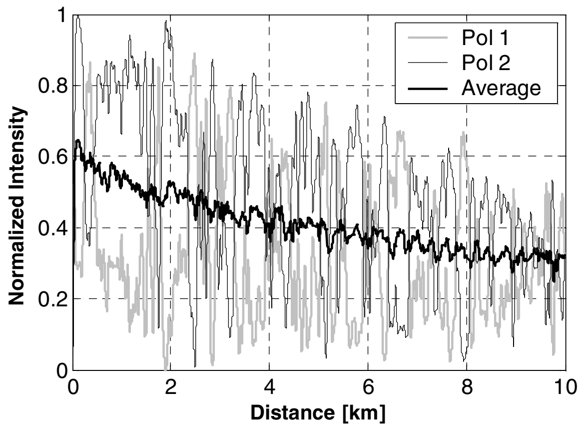

Figure 6. Decoded BOTDA traces for 10 km of fiber, with orthogonally polarized and depolarized probe signals.

as Brillouin loss configurations (changing $g_B(\xi, \ \Delta\nu)$ to $-g_B(\xi, \ \Delta\nu)$) [3], optical pulse coding techniques can in principle be applied to both cases. The first measurements have been carried out to demonstrate the feasibility of using pulse coding techniques in both Brillouin gain and Brillouin loss configurations. In both cases we used 10 km of SSMF and 127-bit Simplex coding with a pulse duration of 10 ns. Every codeword has been averaged eight times, equivalent to ∼1 k averages in the single pulse case. Figure 4 shows the decoded BOTDA traces obtained at a frequency corresponding to the maximum SBS gain when using Brillouin gain configuration (upper trace) and Brillouin loss configuration (lower trace). In both cases, optical pulse coding is successfully applied, obtaining an experimental SNR enhancement of ∼7.1 dB, in agreement with the theoretical value (∼7.5 dB).

Then, measurements over a 50 km SSMF, using both 511-bit Simplex-coded and single-pulsed BOTDA sensors, have been carried out and compared in order to verify the real benefit resulting from coding techniques in long-range BOTDA-based sensors. The comparison between both cases has been done under the condition of similar measurement time, so that every codeword has been averaged four times, equivalent to ∼2 k averages in the conventional case, and corresponding to a measurement time of ∼1 s per frequency step of the reconstructed BGS, excluding processing overhead.

A verification of the effectiveness of polarization scrambling has been carried out and reported in figures 5 and 6, describing BOTDA traces obtained for orthogonal states of polarization for the probe signal. Disconnecting alternatively one of the two branches of the passive PS (shown in figure 3), two BOTDA traces have been measured with orthogonally polarized probe signals as shown in figure 5. For clarity, a zoom of the first kilometers of fiber is shown in figure 6, where, in addition to both traces, we can also observe the effect of the PS when both branches are connected (thick black line in figure 6). The resulting curve is actually equivalent to the average of both orthogonally polarized BOTDA traces, drastically reducing the polarization-induced noise in the final decoded trace. We can thus observe that the passive PS implemented in our setup ensures a uniform scrambling of the probe, avoiding polarization-induced fading in the measured BOTDA traces.

The behavior of the experimentally attained coding gain under similar experimental conditions as in [12] was found equal to ∼10.3 dB, which is in agreement with the expected theoretical value (10.5 dB), allowing us to effectively extend the sensing range by ∼40 km. It is evident from figure 7 that no sensible measurement can be performed over the full 50 km range using 1 m spatial resolution with the conventional sensor, mainly due to the large amount of noise in the measurements. On the other hand, the BGS can be effectively measured, with no distortion, along the 50 km of fiber when using Simplex coding. From the measured BGS, the BFS parameter has then been obtained and shown in figure 7. Calculating the standard deviation of the BFS trace, we can obtain the frequency accuracy of the measurement which is ∼2.2 MHz at 50 km distance in the case of coding. This corresponds to a temperature and strain resolution of ∼2.2 °C and ∼44 $\mu\varepsilon$, respectively. It is important to mention that the conventional BOTDA sensor allows us to obtain the BGS up to ∼30 km distance only, resulting in a completely noisy spectrum for longer distance and making it impossible to retrieve the BFS. Actually, the BFS shown in figure 7 for the single-pulse

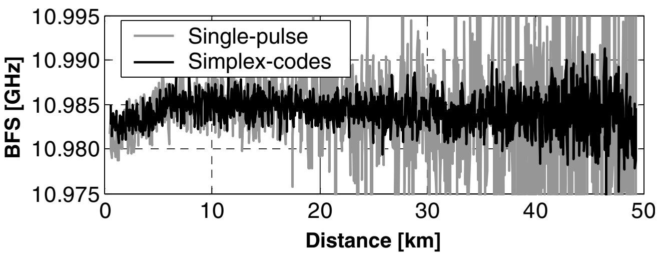

Figure 7. Brillouin frequency shift obtained along 50 km of fiber, for both single-pulse and 511-bit Simplex coding cases.

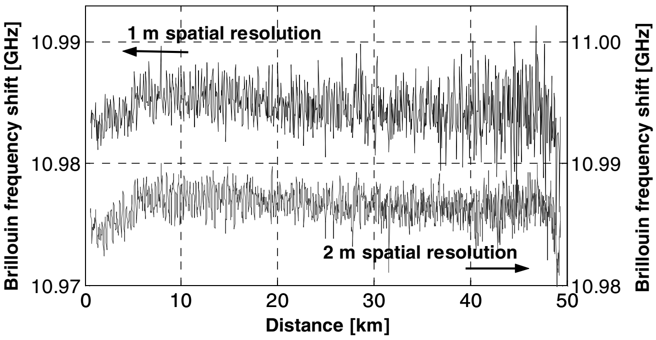

Figure 8. Brillouin frequency shift as a function of distance when using Simplex coding for both 1 m (upper curve and left-side vertical scale) and 2 m spatial resolution (lower curve and right-side vertical scale).

case cannot be employed after 30 km distance, since it only represents the peak value of a noise-dominated spectrum.

The BFS along the 50 km of sensing fiber has also been obtained using 20 ns pulses, allowing for 2 m spatial resolution. In this case 127-bit Simplex coding has been used. Figure 8 shows a comparison when using both 1 m spatial resolution (vertical scale on the left) and 2 m spatial resolution (vertical scale on the right). The shapes of both curves look similar; however, the frequency accuracy in the case of 2 m spatial resolution is found to be equal to ~1.7 MHz, which is equivalent to a temperature resolution of ~1.7 °C and a strain resolution of ~34 $\mu\varepsilon$ at 50 km distance.

One key factor when using coding techniques in long-range BOTDA sensors is to keep linear energy transfer between the probe and pump signals, avoiding nonlinear effects such as pump depletion and modulation instability. For this reason we have carefully investigated those effects in our implemented Simplex-coded sensor. For instance, if pump depletion takes place, the BGS should exhibit a dip lying around the BFS, which has not been observed in our measurements. Moreover, pump depletion should induce a deviation of the measured BFS along the fiber from the real value due to non-local effects, which accumulate and increase with distance. These effects are not present in the measured BFS, as shown in figures 7 and 8. The residual pump variation, measured as the relative change of pump power after propagation along the fiber, with and without SBS interaction, is actually less than 0.7%, confirming negligible pump depletion.

Finally, in order to fully demonstrate the capabilities of optical pulse coding to provide long-range measurements with meter-scale spatial resolution, we have increased the

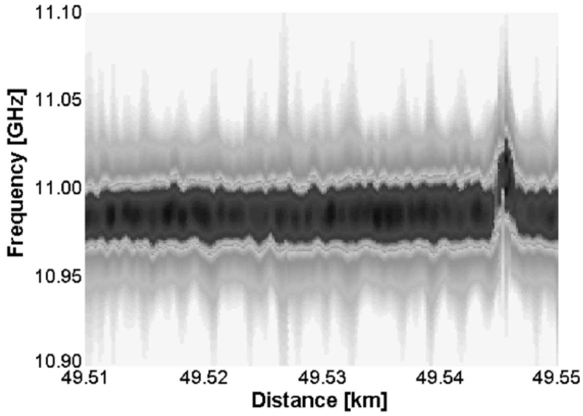

Figure 9. Brillouin gain spectrum obtained near 50 km distance using 511-bit Simplex coding, when 1 m of fiber is heated up to ~50 °C.

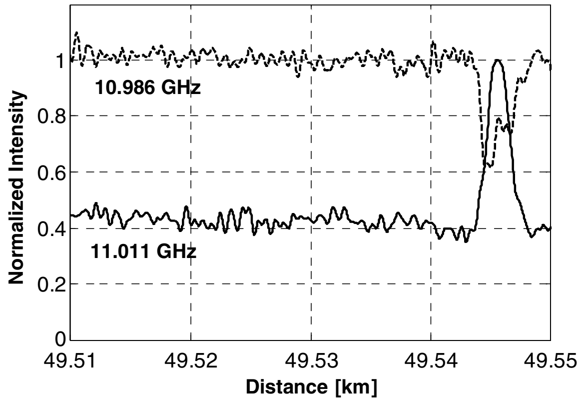

Figure 10. Decoded BOTDA traces obtained at two different frequencies within the BGS when 1 m of fiber is heated up to ~50 °C.

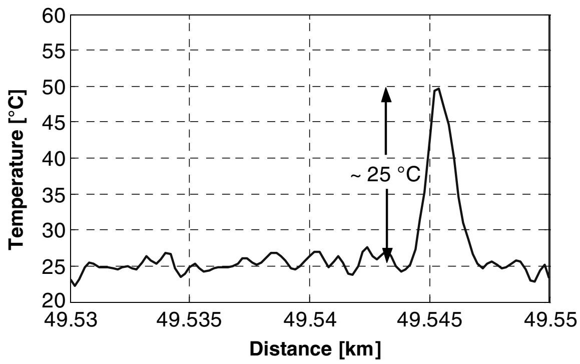

Figure 11. Temperature profile obtained near 50 km distance, when 1 m of fiber is heated up to ~50 °C.

temperature of 1 m of fiber, near 50 km distance, up to 50 °C, while keeping the rest of the fiber at room temperature (25 °C). Figure 9 shows a top view of the BGS along the last few meters of fiber. We can clearly observe the variation of the BGS, and then the BFS, in the heated region. The frequency at the maximum Brillouin gain at room temperature is ~10.986 GHz, while the BFS at 50 °C is ~11.011 GHz. Figure 10 actually shows a detail of normalized BOTDA traces obtained at both frequencies; for the trace taken at

~10.986 GHz we can observe a higher Brillouin gain value along the fiber region placed at room temperature, and a reduced gain value in the heated region. On the other hand, the trace at ~11.011 GHz shows a reduced gain in the fiber at room temperature, while the gain then increases in the region at 50 °C. The measured temperature, obtained from the BFS, near 50 km distance is shown in figure 11, where we can clearly see an ~25 °C temperature variation, corresponding to an ~25 MHz change in the spectrum. This temperature variation has a full width at half maximum (FWHM), representing the real achievable spatial resolution, of ~1.0 m, which demonstrates the potentiality of using optical pulse coding to achieve meter-scale spatial resolution in long-range BOTDA sensors spanning several tens of kilometers.

5. Conclusion

In conclusion, we have theoretically and experimentally demonstrated the feasibility of using optical pulse coding techniques in BOTDA sensors based on either Brillouin gain or Brillouin loss configurations. This technique provides an enhanced SNR when measuring the BGS along the sensing fiber, allowing us to extend the sensing range by ~40 km while maintaining high spatial resolution, without significant modifications of the setup.

References

[1] Horiguchi T *et al* 1995 Development of a distributed sensing technique using Brillouin scattering *J. Lightwave Technol.* **13** 1296–301

[2] Bao X *et al* 1994 Combined distributed temperature and strain sensor based on Brillouin loss in an optical fiber *Opt. Lett.* **19** 141–3

[3] Minardo A *et al* 2005 A reconstruction technique for long-range stimulated Brillouin scattering distributed fibre-optic sensors: experimental results *Meas. Sci. Technol.* **16** 900–8

[4] Nikles M *et al* 1996 Simple distributed fiber sensor based on Brillouin gain spectrum analysis *Opt. Lett.* **21** 758–60

[5] Diaz S *et al* 2008 A high-performance optical time-domain Brillouin distributed fiber sensor *IEEE Sensors J.* **8** 1268–72

[6] Bao X *et al* 1995 Experimental and theoretical studies on a distributed temperature sensor based on Brillouin scattering *J. Lightwave Technol.* **13** 1340–8

[7] Alasia D *et al* 2005 Detrimental effect of modulation instability on distributed optical fiber sensors using stimulated Brillouin scattering *Proc. SPIE* **5855** 587–90

[8] Jones M D 1993 Using simplex codes to improve OTDR sensitivity *IEEE Photon. Technol. Lett.* **15** 822–4

[9] Lee D *et al* 2004 Analysis and experimental demonstration of simplex coding technique for SNR enhancement of OTDR *Proc. IEEE LTIMC (New York, USA, Oct. 2004)* pp 118–22

[10] Soto M A *et al* 2009 Enhanced simultaneous distributed strain and temperature fiber sensor employing spontaneous Brillouin scattering and optical pulse coding *IEEE Photon. Technol. Lett.* **21** 450–2

[11] Soto M A *et al* 2009 Distributed strain and temperature sensing over 50 km of SMF with 1 m spatial resolution employing BOTDA and optical pulse coding *Proc. SPIE* **7503** PDP09

[12] Soto M A *et al* 2010 Simplex-coded BOTDA fiber sensor with 1 m spatial resolution over a 50 km range *Opt. Lett.* **35** 259–61

[13] Linze N *et al* 2009 Signal-to-noise ratio improvement in Brillouin sensing *Proc. SPIE* **7503** 75036F

[14] Minardo A *et al* 2009 A simple technique for reducing pump depletion in long-range distributed Brillouin fiber sensors *IEEE Sensors J.* **9** 633–4